DOI: 10.1002/zaac.200900319

Experimental and Quantum-Chemical Investigations of the UV/Vis Absorption Spectrum of Manganese Carbodiimide, MnNCN

Xiaohui Liu,[a] Richard Dronskowski,*[a] Robert Glaum,[b] and Andreii L. Tchougréeff[c]

Dedicated to Professor Hans-Jörg Deiseroth on the Occasion of His 65th Birthday

Keywords: Carbodiimides; Manganese; Angular overlap model; Effective Hamiltonian crystal field; UV/Vis spectroscopy

Abstract. The UV/Vis absorption spectrum of a single crystal of manganese carbodiimide, MnNCN, has been measured and theoretically analyzed using both the angular-overlap model (AOM) and the effective Hamiltonian crystal field (EHCF) method. Independent from the method used, we find a somewhat higher ligand-field splitting (10 *Dq* ranging from 7300 up to 8842 cm^{-1} depending on the estimation procedure used) compared to Mn–O chromophores and a smaller nephelauxetic ratio (β = 0.62 ÷ 0.67). In addition, the Mn–N bond within the $Mn^{II}N_6$ octahedra is lacking significant π interaction.

Introduction

Despite the fact that calcium cyanamide (or carbodiimide), CaNCN, has been known for at least one century, no cyanamide or carbodiimide of a genuine non-d^{10} magnetic transition metal had ever been synthesized or structurally characterized until recently. On the basis of a large-scale ab initio computational study, however, the complete set of hypothetical *M*NCN phases (*M* = Mn, Fe, Co, Ni, Cu) was predicted in the year 2004 [1]. GGA density-functional theory yielded that all hypothetical *M*NCN phases are unstable in terms of ΔH_f and ΔG_f, and MnNCN was forecast to be the least unstable phase. Shortly after, manganese carbodiimide, MnNCN, was then synthesized by an appropriate metathesis reaction between ZnNCN and $MnCl_2$ [2]. This very first synthesis of a new class of compounds (see below) was then followed by the preparation of single-phase copper carbodiimide, CuNCN, [3] and the synthesis of the isotypical phases nickel carbodiimide, NiNCN, cobalt carbodiimide, CoNCN, [4] and eventually iron carbodiimide, FeNCN [5].

The ultimate motivation for the synthesis of magnetic transition-metal carbodiimides lies in the electronic functionality of the carbodiimide group which can be viewed as a "divalent nitride" or "nitridic pseudo-oxide" anion. Because of the 2– charge of the complex anion and the large electronegativity of the terminal nitrogen atoms, NCN^{2-} clearly resembles O^{2-} despite the fact that its spatial requirement (ca. 24 $cm^3 \cdot mol^{-1}$) is close to the sulfide S^{2-} anion [5,6]. Not too surprisingly, practically nothing is known about the ligating properties of the carbodiimide group, and this is the motivation of the present study.

* Prof. Dr. R. Dronskowski
E-Mail: drons@HAL9000.ac.rwth-aachen.de
[a] Institute of Inorganic Chemistry
RWTH Aachen University
Landoltweg 1
52056 Aachen, Germany
[b] Institut für Anorganische Chemie
Rheinische Friedrich-Wilhelms-Universität
Gerhard-Domagk-Str. 1
53121 Bonn, Germany
[c] Poncelét Laboratory
Independent University of Moscow
Moscow Center for Continuous Mathematical Education
Bolshoi Vlasevsky Per. 11
119002 Moscow, Russia

Experimental Section

The synthesis of MnNCN has been published [2] and starts from a 1:1.2 mixture of ZnNCN and $MnCl_2$ which is ground under a protective argon atmosphere. The mixture is then sealed into a quartz ampoule and heated to 600 °C for three days. Suitable green crystals of MnNCN can be obtained from an additional heat treatment of the product within a LiBr flux at 650 °C. They appear as chemically inert, at least for some days, even when exposed to humid air.

MnNCN is crystal-chemically isotypical with CaNCN, and its structural details are depicted in Figure 1. The terminal nitrogen atoms of NCN^{2-} coordinate the Mn^{2+} as a nearly regular octahedron (6 × Mn–N = 2.26 Å; ∠(N–Mn–N) = 84.1° and 95.9°). Each nitrogen atom is linked to three Mn^{2+} and a carbon atom (∠ (C–N–Mn) = 122.0°; ∠(Mn–N–Mn) = 95.9°). The carbon atom occupies the center of symmetry, so the two nitrogen atoms are generated by one crystallographic site resulting in a perfectly linear carbodiimide $[N{=}C{=}N]^{2-}$ anion with C–N = 1.23 Å.

The single-crystal electronic spectrum of an arbitrary face of a small green crystal (thickness about 0.05 mm) of MnNCN is given in Figure 2. It was measured at ambient temperature using polarized light in a strongly modified CARY 17 microcrystal spectrophotometer (Spectra Services, ANU Canberra, Australia [7]). The spectrometer allows the measurement of polarized spectra of very small single-crystals with diameters down to 0.1 mm. Details on the spectrometer have already

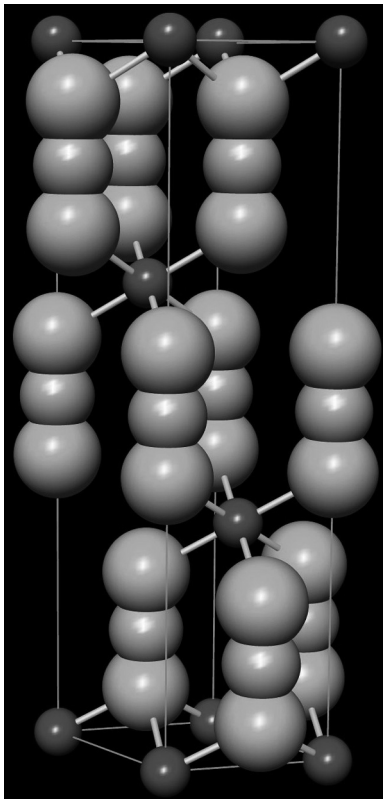

Figure 1. View into the crystal rhombohedral structure of MnNCN showing the octahedral coordination of manganese atoms by nitrogen atoms of the NCN^{2-} carbodiimide groups.

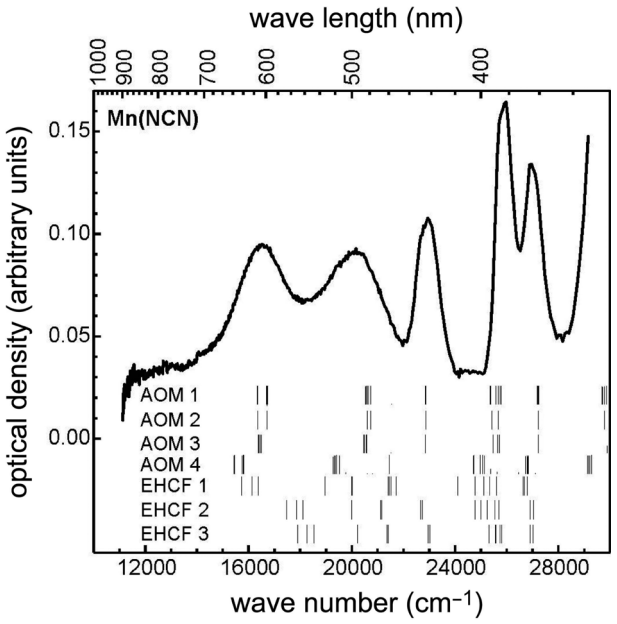

Figure 2. Single-crystal UV/Vis spectrum of MnNCN; crystal thickness about 0.05 mm, cross section 0.3 × 0.1 mm^2. Ticks at the bottom indicate transition energies calculated within the context of AOM and EHCF theories (see text for details).

been described in the literature [8]. Despite its axial space group $R\bar{3}m$, crystals of MnNCN showed no visually detectable dichroic behavior in polarized light under a microscope. Several crystals measured with the direction of the polarized light beam aligned along various directions gave effectively the same absorption spectra, without any hint regarding significant orientation dependence. We therefore waived determination of the polarization direction of the incident light with respect to the crystal axis of the rather small crystals.

A representative experimental absorption spectrum in the UV/Vis region shows quite nicely resolved the typical ligand-field transitions for Mn^{2+} in a weak-field octahedral coordination. The assignment of the transitions using the Tanabe–Sugano diagram for d^5 species [9] is rather straightforward; all corresponding wave numbers are presented in Table 1. All transitions are spin-forbidden and, therefore, weak in intensity. The "horizontal" transitions are free from vibrational broadening and appear as rather sharp signals. By using the Tanabe–Sugano diagram in [9,10] the transition energies lead to the ligand-field splitting 10 Dq = 8840 cm^{-1} and to the Racah parameter B = 753 cm^{-1}. With the free-ion value $B(Mn^{2+})_{f.i}$ = 923 cm^{-1} [11] a nephelauxetic ratio $\beta = B/B(Mn^{2+})_{f.i} = 0.82$ is calculated which is within the range expected for fairly ionic ligands. The use of a more sophisticated analysis of the d-d spectrum suggests, however, much stronger reduction of the Racah parameters (see below).

Angular Overlap Modeling

Manganese carbodiimide is containing trigonally distorted (i.e., slightly compressed) octahedra $[Mn^{II}N_6]$, as seen in Figure 1. For a better understanding of its d-electron energies, calculations within the framework of the *angular overlap model* (AOM) [9, 12, 13] were performed. An advantage of this model is its ability to use the chromophores with their actual structure, as determined from crystal-structure

Table 1. Measured, AOM-fitted and EHCF-calculated transition energies for MnNCN.

	Energy /cm^{-1}				
Transition			EHCF calculated with		
	Measured	AOM AOM 1	fitted B & C EHCF 1	extracted B & C (method I) EHCF 2	extracted B & C (method II) EHCF 3
$^6A_{1g} \rightarrow {}^4T_{1g}(G)$	16470	16330–16732	15711–16374	17474–18110	17890–18520
$^6A_{1g} \rightarrow {}^4T_{2g}(G)$	20170	20520–20727	18958–20015	19987–21157	20200–21408
$^6A_{1g} \rightarrow {}^4A_{1g}(G)$	22710[a)]	22838–22855	21393	22650	22944
$^6A_{1g} \rightarrow {}^4E_g(G)$	23020		21457–21459	22718–22720	23013–23015
$^6A_{1g} \rightarrow {}^4T_{2g}(D)$	25890	25355–25772	24776–25331	25241–25697	25313–25736
$^6A_{1g} \rightarrow {}^4E_g(D)$	27040	27172–27227	26673–26787	26910–27026	26906–27022

a) = Shoulder.

Zeitschrift für anorganische und allgemeine Chemie ZAAC Journal of Inorganic and General Chemistry

analysis. In AOM instead of using global parameters, such as 10*Dq* or Δ_o, one σ- and two π-interactions (in total 18 bonding parameters for an octahedral chromophore) of each ligand with the five 3d orbitals of the central ion are used for the fitting between calculated and observed transition energies. This decomposition of the global ligand-field parameter into parameters describing individual bonding interactions permits also accounting for second-sphere ligand-field effects [14], e.g., cation-cation interaction or misdirected valence behavior. To reduce the number of independent bonding parameters, constraints between some of them may be introduced. Thus, for the energy $e_\sigma(M–L)$, a proportionality to the distance going as $d(M–L)^{-5.0}$ may be assumed [9,15]. In general, the energy of e_π is set to one quarter of the corresponding energy e_σ in the case of "undisturbed" π-interaction [9,17]. In the case of the particular bonding situation encountered in the carbodiimide, $e_\pi \approx 0$ was assumed. The validity of this assumption will be discussed.

Interelectronic repulsion is introduced into the AOM calculations via the Racah parameters *B*, *C*, and the Trees correction $\alpha L(L+1)$ [18], spin-orbit coupling by ξ. For the angular overlap modeling the free ion ratio $C_0/B_0 = 3.5$ for Mn^{2+} was used and only slightly modified during the fitting procedure [11]. Variation in the covalency of the Mn–N interaction was considered by variable nephelauxetic ratios β ($\beta = B/B_0$; $B_0(Mn^{2+}) = 923$ cm^{-1} [11]). The spin-orbit coupling parameter ξ was also assumed to be reduced relative to the free ion value $\xi_0(Mn^{2+}) = 300$ cm^{-1} [9] according to β. For the AOM calculations the PC program CAMMAG [16] in a modified version [19] was used.

Quantum-Chemical Investigation

The AOM fitting can be compared with the quantum-chemical modeling of the d^5-chromophore performed with use of the Effective Hamiltonian Crystal Field (EHCF) method [20]. It allows for the direct semi-empirical calculation of the crystal field felt by the d-shell of a transition-metal ion in the complex or solid on the basis of composition and geometry with a minimal fit of parameters used (see below). The EHCF method attributes the observed splitting dominantly (up to 90 % [20]) to the contribution of the one-electron transfers between the d-shells which are partially filled by an integer number of electrons and the MOs (both occupied and vacant) of the ligands. This result is reached by assuming the many-electron wave function of a transition-metal complex in the form

$\Psi = \Phi_d\,(n_d) \wedge \Phi_L\,(n_l)$

where Φ_d is the full configuration-interaction function of n_d electrons in the d-shell of the transition-metal ion and Φ_L is the function of all other (n_l) electrons of the system taken in a semiempirical self-consistent field approximation; the symbol ∧ refers to the fact that the above "product" function is antisymmetric (i.e., changes its sign) when the coordinates of each pair of n_d+n_l electrons are interchanged. This type of the wave function formalizes the usual assumptions of the crystal field and AOM theories but it is approximate because the Hamiltonian of the transition-metal complex always contains resonance terms, responsible for one-electron transfers between the d-shell and the rest of the complex molecule, thus destroying the above form of the wave function in a precise sense. This form can be, however, conserved provided the aforementioned one-electron transfers are treated by a sort of perturbation theory. This yields the following form of the effective Hamiltonian for the d-shell:

$H_d^{eff} = H_{field} + H_{Coul}$

In the above expression the term H_{Field} stands for the one-electron operator describing interactions of the electrons in the d-shell with the atomic core of the transition metal ion and the entire surrounding of the d-shell. The operator H_{Coul} is the two-electron operator describing the Coulomb interactions between the d-electrons. The matrix elements of the operator H_{Field} are contributed by the ionic and covalent parts of the effective crystal field ($W^{ion}{}_{\mu\nu}$ and $W^{cov}{}_{\mu\nu}$, respectively) calculated from the semiempirical self-consistent field wave function Φ_L according to the formulae:

$$W_{\mu\nu}^{ion} = \sum_L V^L{}_{\mu\nu} Q_L + \sum_{i \in 4s,4p} g_{\mu i} P_{ii}$$

$$W_{\mu\nu}^{cov} = \sum_{j \in MO} \eta_{\mu j} \eta_{\nu j} \left(\frac{n_j/2}{\Delta E_{jd}} - \frac{1 - n_j/2}{\Delta E_{dj}} \right).$$

Here, n_j is the occupation number of the j-th ligand MO in the single-determinant wave function Φ_L equal to 2 or 0, $\eta_{\mu i}$ is the one-electron hopping integral between the μ-th d-AO and j-th ligand MO, ΔE_{jd} (ΔE_{dj}) are the energies of the states with one electron transferred between the d-shell and the j-th ligand MO, calculated according to the formulae:

$$\eta_{\mu i} = \sum_l c_{il} \eta_{\mu l}$$
$$\eta_{\mu l} = \eta (\eta_d + \eta_l) S_{\mu l}$$
$$\Delta E_{jd} = -\varepsilon_j - A_d - g_{dj}$$
$$\Delta E_{dj} = I_d + \varepsilon_j - g_{dj}$$

Here, the ε_j's are the orbital energies of the ligand MOs, A_d and I_d are, respectively, the electron affinity and the ionization potential of the d-shell estimated as free-ion values shifted by the Coulomb field of the effective charges in the ligands, and the c_{il}'s are the molecular-orbital LCAO coefficients from the semi-empirical self-consistent field calculation for the wave function Φ_L. The quantities η_d and η_l are the hopping parameters characteristic for the given transition-metal atom and given organogenic donor atom separately; $S_{\mu l}$ are the overlap integrals, stipulated by chemical composition and molecular arrangement, between the μ-th d-orbital of the metal ion and the *l*-th AO of the ligands. The parameter $\eta = \eta$(Mn–N) – generally specific for a pair of the transition-metal atom and the organogenic donor atom – scales the one-electron hopping $\eta_{\mu l}$ integrals between the d-shell of manganese and the orbitals *l* located on the nitrogen donor atoms (Note that this parameter scaling the one-electron hopping is usually dubbed as β in the quantum-chemical literature. In order to avoid confusion with the nephelauxetic ratio β, however, we use a different naming convention (η) in this very manuscript.). The quantities g_{dj} are the energies of the Coulomb interaction between electron and hole located in the d-shell and the j-th ligand MO. The matrix elements of the operator H_{Coul} are calculated from the Racah parameters *B* and *C*, which are renormalized in the crystal (or complex) as compared to their free ion values due to the nephelauxetic effect.

By using the EHCF theory, the effective crystal field felt by the d-shell in each coordination compound is explicitly *calculated* on the basis of the structure and composition of the compound at hand. It has been shown [20, 21, 27–36] that namely the hopping integrals together with the energies of the states with electrons transferred to (from) the d-shell and from (to) the ligands ("charge-transfer states") contribute up to 90 % of the observed splitting; the rest is given by the Coulomb field of the effective charges in the ligands. These quantities are uniquely defined by the chemical composition and by the molecular

spatial structure. This specificity is explicitly reflected by the values of the MO-LCAO coefficients of the *l*-system c_{il}, of the orbital energies ε_j of the latter, as well by the (geometry-dependent) overlap integrals $S_{\mu d}$, quantities η_d and η_l having the dimension of energy, and the scaling factor $\eta = \eta^{ML}$ together defining the hopping matrix elements characteristic for the given transition-metal atom and given ligands.

In the solid-state context pertinent to the current study, the EHCF method has been employed in its cluster version in which the d-chromophore of interest is supplied by a ligand sphere represented by a structural cut taken from the crystal. In this study, we employed a cluster model containing 31 atoms, that is, seven Mn^{2+} ions and 24 N/C atoms forming eight $[N=C=N]^{2-}$ groups with an overall cluster charge of –2.

The value of the scaling parameter η was determined from the fitting of the d–d spectrum of Mn-porphyrin (η(Mn–N) = 1.32) [21] with all other parameters fixed at their standard values as accepted in [20]. The methodology by which the scaling factor $\eta = \eta^{ML}$ can be determined from one known complex containing the specified pair of transition-metal atom *M* and a donor atom *L* and then used in whatever complex of the same metal with any ligand with the same donor atom is thoroughly tested in numerous publications (see Refs. [21, 27–36]). Under these conditions the crystal field was computationally found for the Mn d-shell and further used for calculating its d–d excitation spectrum.

Results

Angular Overlap Model

The AOM method can be used both in the sense of the direct (the parameters are given – a spectrum is calculated) and the inverse (a spectrum is given – the parameters are fitted) problems. In this paper it is used in the inverse problem context. At the first step of the fitting procedure, the energy for the $^6A_{1g} \rightarrow {}^4A_{1g}$(G) transition was reproduced by a variation of *B*. In the second step, a satisfactory match between theoretical and observed transition energies for the rest of the absorption bands was reached by adjusting e_σ(Mn–N). Using e_σ(Mn–N) = 2600 cm^{-1}, e_π(Mn–N) = 0 cm^{-1}, *B* = 766 cm^{-1} (*C*/*B* = 3.6, β = 0.83), α = 70 cm^{-1}, and ξ = 249 cm^{-1}, this eventually allowed a reasonable fit (Table 1, Figure 2, "AOM 1"). AOM calculations using the same parameterization, but setting ξ = 0 cm^{-1} produce basically the same transition energies (Figure 2, "AOM 2"), thereby showing the rather small influence of spin-orbit coupling on the splitting of the states. For calculation "AOM 3" (Figure 2) O_h symmetry of the chromophore was assumed, maintaining the same parameterization as for "AOM 1". Comparison of "AOM 1" with "AOM 3" nicely shows the influence of the trigonal distortion of the chromophore on the splitting of the states. It is quite remarkable that calculation "AOM 4", which is similar to "AOM 1" but without the Trees correction (α = 0), compares fairly well with calculation "EHCF 1" (see below).

Effective Hamiltonian Crystal Field

The EHCF method is largely used in the direct problem context: the chemical composition and the structure of the complex (or crystal) are given which are used to calculate, first, the crystal field matrix (operator H_{Field}) and, second, by using the Racah parameters, the spectrum. The results of our calculations as presented in Figure 2 (EHCF1, EHCF2, and EHCF3) show that the calculated field has a much lower symmetry than that of an octahedron, which is not surprising. The e_g and t_{2g} manifolds are, in fact, not precisely degenerate but considerably split by ca. 1000 ÷ 1500 cm^{-1}. The value of 10 *Dq* (taken as a splitting between the average energies of the three lower, quasi t_{2g} d-levels, and the two higher, quasi e_g d-levels) then becomes 7300 cm^{-1}, to be compared with 7800 cm^{-1} coming from the above AOM fit according to the relation: 10 *Dq* = $3e_\sigma$(Mn–N) – $4e_\pi$(Mn–N) [9,22]. The additional splitting of the e_g and t_{2g} manifolds appears because of the fact that the closest ligand arrangement is not ideally octahedral due to the spatial extension of the $[N=C=N]^{2-}$ groups. In addition, because of the lack of the true octahedral symmetry and because of the lack of the axial symmetry of the Mn–N bonds, all ligand orbitals contribute to the crystal field so that some π-interactions are included. More detailed account for the actual geometry and electronic structure of the ligands by the EHCF method explains the much stronger splitting between the states in the approximate octahedral multiplets in all EHCF calculations as given in Figure 2 as compared to the AOM calculations. Another piece of variance between these two methods is that the EHCF so far does not take into account the spin-orbit interaction. However, as evidenced by a comparison between the results of the "AOM2" and "AOM3" calculations, the splitting caused by the latter is of minor importance for the present case. Finally, the calculation "AOM4" performed with no Trees correction fairly coincides with the "EHCF1" (which also does not include the latter) performed with the same values of the Racah parameters.

Despite the differences in the crystal fields coming from the AOM fit and from the semiempirical EHCF calculation, the experimental spectroscopic data are fairly reproduced by both of them. If the AOM-fitted values of *B* = 766 cm^{-1} and *C* = 3.6 × *B* = 2760 cm^{-1} are used as well in the EHCF calculation (Figure 2, "EHCF 1"), the first transition occurs at 16127 cm^{-1} (here, an average of three close transition energies is taken, as well as in other relevant cases below), to be compared with the experimental value of 16472 cm^{-1}. An alternative might be to extract the values of *B* and *C* immediately from the experiment using the exact (within the crystal-field theory) expressions for the energies of the two ^4E_g(G) and ^4E_g(D) states available: $E(^4E_g(G)) = 10\ B + 5\ C$ and $E(^4E_g(D)) = 17\ B + 5\ C$ [23]. The energy difference between them is just 7 *B*, which allows one to extract the experimental estimates for *B* and *C*.

The available experimental data, however, admit a twofold interpretation since it is not clear a priori whether the shoulder at 22712 cm^{-1} must be interpreted as a transition to the ^4E_g(G) or to the $^4A_{1g}$(G) state. By assuming the shoulder to be the transition to the ^4E_g(G) state, one results at the following estimates (further referred to as "extracted by method I", calculation "EHCF2") of the Racah parameters: *B* = 618 cm^{-1} and *C* = 3303 cm^{-1}. The alternative assignment of the above transitions yields the following estimates (referred to as "extracted by method II", calculation EHCF3"): *B* = 575 cm^{-1} and *C* =

Zeitschrift für anorganische und allgemeine Chemie ZAAC Journal of Inorganic and General Chemistry

3453 cm^{-1}. The fact that the ratios *C*/*B* for both "extracted" sets of Racah parameters are much closer to their traditional values (5.35 and 6.00, respectively) than that coming from the AOM-based fit is remarkable enough. Indeed, the ratio from the AOM-based fit indirectly admits that the nephelauxetic effect for the Racah parameter *C* is, for some reason, about as strong as that for the *B* parameter, in contrast with the major body of the known data [24] and the recent theoretical estimates [25], which unequivocally establish that the *C*/*B* ratio *must* be significantly larger in the complex than in the free ions (where it theoretically is about four and experimentally always larger than four) due to considerably stronger nephelauxetic effect for the *B* parameter than for the *C* parameter. For the "extracted" data I and II the nephelauxetic ratios β are 0.623 and 0.669, respectively, indicating much stronger renormalization of the interactions of d-electrons in the presence of presumably highly polarizable $[N=C=N]^{2-}$ dianions than what follows from the AOM fit.

Table 1 further evidences that, in general, the calculation "EHCF 1" (Figure 2) using the AOM-fitted values of the Racah parameters better reproduces the energies of the first two transitions, but underestimates the positions of the ^4E_g(G) and $^4A_{1g}$(G) and $^4T_{2g}$(D) states. The energies of these states as well of the higher excitations come out more realistically if either of the extracted sets of the Racah parameters is used in the EHCF context (EHCF 2 and EHCF 3). This is purchased by a somewhat larger error in estimating the first transition. Nevertheless, the EHCF 2 procedure (with *B* and *C* extracted by method I) gives the error of only ca. 1200 cm^{-1} for the first transition and much smaller ones for all other transitions, thereby producing the most balanced description of the spectrum (direct problem) of those presented in this paper.

Discussion

For the first time a homoleptic complex of the carbodiimide ligand with a transition metal has been spectroscopically characterized. The UV/Vis spectrum of MnNCN shows surprising similarity to the one reported for $[Mn(en)_3](NO_3)_2$ [26]. The ligand-field splitting extracted by AOM for MnNCN is about 10 % *higher* than typically found for $[Mn^{II}O_6]$ chromophores, e.g., in anhydrous phosphates [10]. Compared to the oxo-chromophores both the AOM- and Tanabe–Sugano-derived nephelauxetic ratios are *smaller* (0.83 instead of 0.93). This finding is also corroborated from a quantum-chemical EHCF study, but with even smaller nephelauxetic ratios (0.62 and 0.67). Thus, both 10 *Dq* and β nicely fit into a picture with a *more covalent* Mn–N bond compared to the Mn–O interaction. The higher 10 *Dq* is probably caused by the lack of π-interaction between Mn and N. The interpretational difference between the AOM and EHCF modeling is that, as seen from the EHCF perspective, the difference of the 10 *Dq* values in the $[MnO_6]$ and $[MnN_6]$ chromophores is attributable to the specific values of both the Mn–O and Mn–N one-electron hopping integrals and to the lower energy of the ligand to metal charge-transfer states in the case of carbodiimide, which both suggest somewhat stronger covalency in the EHCF context. As for the nephelauxetic parameters, the simple crystal-field formulae for energies of the ^4E_g(G) and ^4E_g(D) states and some considerations based on the general theory of the nephelauxetic effect [25] yield *two* more systems of "extracted" Racah parameters, both being almost equally acceptable in terms of reproducing the observed spectra. They both better fit to the general theory of the d-d-spectra, in particular concerning the *C*/*B* ratio for the renormalized parameters. One should not understand the smaller value of the nephelauxetic ratio as an indication of some particularly strong covalency suggested by the EHCF itself and by the extraction schemes based on it. By contrast, stronger renormalization of the Racah parameters (small values of the nephelauxetic ratios) rather indicate to a stronger polarizability of the ligand environment in the studied compound which puts the $[N=C=N]^{2-}$ ligand among those with relatively weak crystal field in the spectrochemical series, but among those with the strong nephelauxetic effect in the nephelauxetic series – a situation quite well known in the literature.

Acknowledgement

It is a pleasure to thank *Deutsche Forschungsgemeinschaft* for financial support, in particular regarding the visit of ALT to the Institute of Inorganic Chemistry at RWTH Aachen University through grant No. DR342/18–1. In addition, we acknowledge the *Russian Foundation for Basic Research* for the financial support dispatched to ALT through grant No. 07–03–01128.

References

[1] M. Launay, R. Dronskowski, *Z. Naturforsch.* **2005**, *60b*, 437.
[2] X. Liu, M. Krott, P. Müller, C. Hu, H. Lueken, R. Dronskowski, *Inorg. Chem.* **2005**, *44*, 3001.
[3] X. Liu, M. A. Wankeu, H. Lueken, R. Dronskowski, *Z. Naturforsch.* **2005**, *60b*, 593.
[4] M. Krott, X. Liu, B. P. T. Fokwa, M. Speldrich, H. Lueken, R. Dronskowski, *Inorg. Chem.* **2007**, *46*, 2204.
[5] X. Liu, L. Stork, M. Speldrich, H. Lueken, R. Dronskowski, *Chem. Eur. J.* **2009**, *15*, 1558.
[6] L. Stork, X. Liu, B. P. T. Fokwa, R. Dronskowski, *Z. Anorg. Allg. Chem.* **2007**, *633*, 1339.
[7] E. Krausz, *AOS News* **1998**, *12*, 21.
[8] E. Krausz, *Aust. J. Chem.* **1993**, *46*, 1041.
[9] B. N. Figgis, M. A. Hitchman, *Ligand Field Theory and Its Applications*, Wiley-VCH, New York, **2000**.
[10] R. Glaum, H. Thauern, A. Schmidt, M. Gerk, *Z. Anorg. Allg. Chem.* **2002**, *628*, 2800.
[11] D. Reinen, G. Schwab, V. Günzler, *Z. Anorg. Allg. Chem.* **1984**, *516*, 140.
[12] C. K. Jørgensen, R. Pappalardo, H. H. Schmidtke, *J. Chem. Phys.* **1963**, *39*, 1422.
[13] D. E. Richardson, *J. Chem. Educ.* **1993**, *70*, 372.
[14] D. Reinen, M. Atanasov, S. L. Lee, *Coord. Chem. Rev.* **1998**, *175*, 91.
[15] M. Bermejo, L. Pueyo, *J. Chem. Phys.* **1983**, *78*, 854.
[16] D. A. Cruse, J. E. Davies, J. H. Harding, M. Gerloch, D. J. Mackey, R. F. McMeeking, "*CAMMAG*", a FORTRAN program, Cambridge, **1980**.
[17] M. Gerloch, "*Magnetism and Ligand Field Theory*", Cambridge Univ. Press, **1983**.
[18] R. E. Trees, *Phys. Rev.* **1951**, *83*, 756; R. E. Trees, *Phys. Rev.* **1951**, *84*, 1089.
[19] M. Riley, "*CAMMAG for PC*", V 4.0, Univ. of Queensland, St. Lucia, Australia, **1997**.

[20] A. V. Soudackov, A. L. Tchougréeff, I. A. Misurkin, *Theor. Chim. Acta* **1992**, *83*, 389.
[21] A. M. Tokmachev, A. L. Tchougréeff, *Khim. Fiz.* **1999**, *18*, *Chem. Phys. Rep.* **1999**, *18*, 163.
[22] A. B. P. Lever. "*Inorganic Electronic Spectroscopy*", Elsevier: Amsterdam, **1984**.
[23] J. S. Griffith. "*The Theory of Transition Metal Ions*", Cambridge, **1961**.
[24] I. B. Bersuker. "*Electronic Structure and Properties of Coordination Compounds*", Khimiya, Moscow, **1976**.
[25] A. L. Tchougréeff, R. Dronskowski, *Int. J. Quantum Chem.* **2009**, *109*, 2606.
[26] R. A. Palmer, M. C.-L. Yang, J. C. Hempel, *Inorg. Chem.* **1978**, *17*, 1200.
[27] A. V. Soudackov, A. L. Tchougréeff, I. A. Misurkin, *Zh. Fiz. Khim.* **1994**, *68*, *Russ. J. Phys. Chem.* **1994**, *68*, 1135.
[28] A. V. Soudackov, A. L. Tchougréeff, I. A. Misurkin, *Zh. Fiz. Khim.* **1994**, *68*, *Russ. J. Phys. Chem.* **1994**, *68*, 1142.
[29] A. V. Soudackov, A. L. Tchougréeff, I. A. Misurkin, *Int. J. Quantum Chem.* **1996**, *57*, 663.
[30] A. V. Soudackov, A. L. Tchougréeff, I. A. Misurkin, *Int. J. Quantum Chem.* **1996**, *58*, 161.
[31] A. L. Tchougréeff, *J. Mol. Catal.* **1997**, *119*, 377.
[32] A. L. Tchougréeff, *Khim. Fiz.* **1998**, *17*, *Chem. Phys. Reports.* **1998**, *17*, 1241.
[33] A. V. Sinitsky, M. B. Darkhovskii, A. L. Tchougréeff, I. A. Misurkin, *Int. J. Quantum Chem.* **2002**, *88*, 370.
[34] A. M. Tokmachev, A. L. Tchougréeff, *J. Sol. State Chem.* **2003**, *176*, 633.
[35] M. B. Darkhovskii, A. V. Soudackov, A. L. Tchougréeff, *Theor. Chem. Acc.* **2005**, *114*, 97.
[36] M. B. Darkhovskii, A. L. Tchougréeff in: "*Molecular modeling of metal complexes with open d-shell*." in "*Recent Advances in Theory of Chemical and Physical Systems*" (Eds.: J.-P. Julien, J. Maruani, E. Brandas), **2006**, Kluwer, Dordrecht.

Received: June 30, 2009
Published Online: December 17, 2009

